A Hydrogen Maser at Temperatures Below 1 K

ROBERT F. C. VESSOT, EDWARD M. MATTISON, RONALD L. WALSWORTH, JR., ISAAC F. SILVERA, HERMAN P. GODFRIED, AND CHARLES C. AGOSTA

Abstract—**We describe a hydrogen maser oscillator that has been designed to operate as a highly stable clock operating at temperatures below 1 K using a film of superfluid helium 4 as a storage volume wall coating. We derive the expressions that predict the statistically determined frequency stability of the maser in terms of the maser's internal parameters. Our design follows conventional atomic beam state selection techniques for supplying atoms in the $F = 1$, $m_F = 0$ hyperfine sublevel to the oscillating region, which is located inside a sapphire dielectrically loaded TE_{011}-mode cavity resonator. Measurements of the Hydrogen–Helium wallshift and the line Q of the maser oscillator have been made with unsaturated superfluid helium films at temperatures between 0.475 and 0.575 K. These show that the wallshift depends strongly on film thickness and that the Q of the maser oscillator improves very rapidly as film thickness is increased.**

I. Introduction

SINCE the invention of the atomic hydrogen maser in 1960 by Kleppner, Goldenberg, and Ramsey [1] there has been an increasing level of activity in the search for improvement of the maser's hydrogen storage technique. The ability to keep a constantly replenished quantity of hydrogen atoms localized for extended times in a region where they are exposed to a uniform, constant-phase RF magnetic field oscillating at the hyperfine resonance frequency results in a narrow oscillator linewidth, which is the principal reason for the success of the hydrogen maser as a very high stability oscillator. In the maser a beam of hydrogen atoms in the two upper hyperfine energy levels ($F = 1$, $m_F = 0$, and $m_F = 1$) is state selected by a strong, inhomogeneous magnetic field. The state-selected beam is directed into the storage region, where atoms in the $F = 1$, $m_F = 0$ state undergo stimulated transitions to the $F = 0$, $m_F = 0$ state, coherently contributing energy to the RF magnetic field. The stored atoms move at thermal velocities associated with the temperature of the boundaries of the storage region (which for historical reasons is often referred to as the storage "bulb"). The linewidth Δf of the released energy depends on the length of time Δt the atoms are exposed to the RF field in an unperturbed manner, as described by the Heisenberg uncertainty principle, $\Delta E \Delta t \sim h$ (or $\Delta f \Delta t \sim 1$). Here $E = hf$ is the energy of the hyperfine separation, h is Planck's constant, and f is the frequency of the transition.

The key to the whole process is the ability of the storage region walls to reflect the incoming atoms without excessively distributing the phase of their oscillating dipole moments. Usually the dimensions of the bulb are commensurate with half the 21-cm wavelength of oscillation. At room temperature a typical atom collides with the wall 3×10^4 times per second. The velocity of impact is about 3.6 km/s. That any surface material can make possible such collisions without disrupting the phase of the atom's oscillating dipole moment is indeed remarkable.

The first wall coatings used in room-temperature masers were of dimethyl-dichlorosilane, and later Teflon was (and still is) used. The possibility of low-temperature operation of hydrogen masers arose in 1977; about this time the suggestion was made by Shapiro [2] that considerable advantage to hydrogen masers might result in such low-temperature operation if suitable wall surfaces could be found. Crampton, Phillips, and Kleppner [3] described the advantages resulting from low thermal noise, and the mechanical, thermal, and magnetic stability of materials. The situation was very tempting indeed, if only the wall question could be resolved. Attempts to use frozen-in-place coatings of CF_4 at about 35 K [4] and neon at about 6 K [5] have been made, but these do not appear to have much promise for highly stable oscillators.

In order to understand how low-temperature operation can improve the frequency stability of the hydrogen maser, we examine the Allan variance [6] σ of the maser's frequency fluctuations. We express the Allan variance, which is a function of the maser's power output, oscillation line Q, receiver noise figure and bandwidth, and temperature [7], [8] in terms of the maser's oscillation parameter q [9].

Following Vessot *et al.* [10] and Berlinsky and Hardy [11], we recognize two major contributions to instability that result from thermal noise:

1) Noise within the bandwidth of the receiver system, including the excess noise of the first amplifier stages.
2) The thermal noise within the oscillation linewidth, which defines the Q of the atomic system. This noise is a fundamental performance limit.

The observed frequency pulling, owing to mistuning of the cavity resonator, can also be included in a statistical sense by postulating that the spectrum, $S_y(f)$, of the cav-

Manuscript received June 23, 1986. This work was supported in part by the Smithsonian Institution's Scholarly Studies and Research Opportunities Fund and the Department of Energy under Grant DE-FG02-85ER45190.

R. F. C. Vessot and E. M. Mattison are with Harvard-Smithsonian Center for Astrophysics, Cambridge, MA 02138.

R. L. Walsworth, Jr., I. F. Silvera, H. P. Godfried, and C. C. Agosta are with Lyman Laboratory of Physics, Harvard University, Cambridge, MA 02138.

IEEE Log Number 8613613.

0018-9456/87/0600-0588$01.00 © 1987 IEEE

Authorized licensed use limited to: University of Maryland College Park. Downloaded on November 29,2021 at 12:22:24 UTC from IEEE Xplore. Restrictions apply.

ity offset frequency follows some combination of $1/f$ (flicker of frequency) and $1/f^2$ (random walk of frequency) distribution [12] and can, therefore, be characterized by an Allan variance $\sigma_c(\tau)$.

The expression describing the stability is given by

$$\sigma^2(\tau) = kT\left(\frac{FB}{P_0\omega_0^2}\frac{1}{\tau^2} + \frac{1}{2Q_l^2P}\frac{1}{\tau}\right) + \sigma_c^2(\tau)\frac{Q_c^2}{Q_l^2}. \quad (1)$$

Here k is Boltzmann's constant, T is the physical temperature, assumed to be uniform throughout the system, F is the noise figure of the receiver and B its noise bandwidth, $\omega_0 = 2\pi f_0$ is the angular frequency of oscillation, P_0 is the power delivered to the receiver, P is the power delivered to the cavity by the atoms, and Q_c is the loaded Q of the cavity resonator. The oscillating line Q of the atomic resonance is given by $Q_l = \omega/2\gamma_{2T}$, where γ_{2T} is the total transverse (dephasing) relaxation rate, which will be discussed later.

We can express (1) in terms of the internal parameters of the maser as defined by Kleppner *et al.* [9]. The relationship between the power P, radiated by the hydrogen atoms, and the flux I, of atoms in the $F = 1$, $m_F = 0$ state entering the storage volume, can be expressed in terms of the maser's oscillation parameter q, defined by

$$q = \frac{\hbar}{8\pi\mu_0^2}\frac{I_{\text{total}}}{I}\left(1 + \frac{\gamma_w}{\gamma_b}\right)\frac{V_c}{\eta V_b}\frac{\sigma_{se}(T)\,\bar{v}_r(T)}{Q_c}.$$

Fig. 1, from Kleppner *et al.*, shows how the quantity

$$\frac{P}{P_c} = -2q^2\left(\frac{I}{I_{\text{th}}}\right)^2 + (1 - 3q)\frac{I}{I_{\text{th}}} - 1$$

behaves in terms of the parameter q. Here

$$P_c = \frac{\omega\hbar^2V_c(\gamma_b + \gamma_\omega)^2}{8\pi\mu_0^2Q_c\eta}$$

$$I_{\text{th}} = 2P_c/\hbar\omega.$$

γ_w is the dephasing relaxation rate of atoms from wall collisions and γ_b is the loss rate of atoms from the storage bulb. We assume here that γ_b is due to all mechanisms causing loss of atoms, including recombination on the storage bulb walls as well as escape through the bulb's entrance aperture. We assume that the rate of loss of polarization and the rate of dephasing owing to wall collisions are equal. Atoms in the storage bulb will also suffer dephasing resulting from spin–exchange collisions. The rate $\gamma_{\text{se}} = n\bar{v}_r\sigma_{\text{se}}$ of such collisions is governed by the atomic density n, the spin–exchange cross section $\sigma_{\text{se}}(T)$, and the relative atomic velocity $\bar{v}_r(T) = 4(kT/\pi m)^{1/2}$. The total transverse relaxation rate is given by $\gamma_{2T} = \gamma_b + \gamma_w + \gamma_{\text{se}}$. The quantity V_c/V_b is the ratio of the resonant cavity volume to the storage volume. $\eta = \langle H_z\rangle_b^2/\langle H^2\rangle_c$ is the filling factor representing the ratio of the RF magnetic field engaged in the transition, to the total RF magnetic field in the resonant cavity. I_{tot} is the total flux of atoms entering the bulb (which, under the usual state-selection conditions, is twice the flux I in the desired $F = 1$, $m_F = 0$ state) and μ_0 is the Bohr magnetron.

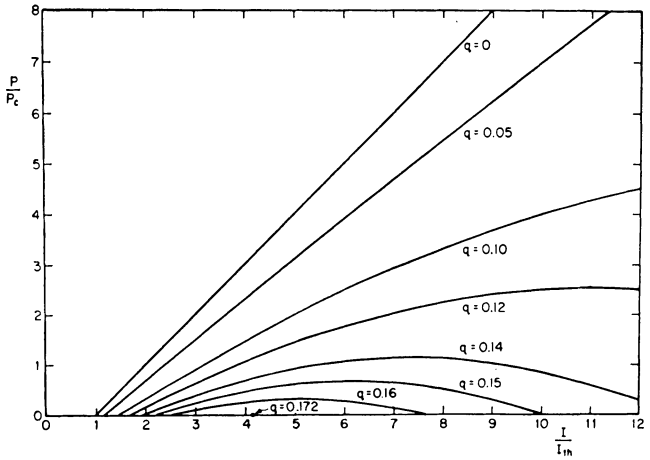


Fig. 1. P/P_c versus I/I_{th} for different values of the parameter q[9].

We note that the quadratic behavior of power with beam flux results from spin–exchange quenching. The parameter q expresses the specific conditions inherent in the maser's design and operating temperatures; for oscillation to occur, q must be less than 0.172.

We can recast (1) in terms of q and the beam flux I by substituting the appropriate relationship for Q_l and output power. The line Q can be expressed by

$$Q_l \equiv \frac{\omega}{2\gamma_{2T}} = \frac{\omega}{2(\gamma_b + \gamma_w)}\left(1 + q\frac{I}{I_{\text{th}}}\right)^{-1}. \quad (2)$$

The three noise contributions, which include the assumed spectral behavior of the resonator frequency variations $\sigma_c(\tau)$, then appear as follows:

$$\sigma^2(\tau) = \frac{\frac{8\pi\mu_0^2}{\omega^3\hbar^2}\frac{FkTB\eta}{V_c}\frac{Q_{\text{ext}}}{(\gamma_b + \gamma_w)^2}}{-1 + (1 - 3q)\frac{I}{I_{\text{th}}} - 2q^2\left(\frac{I}{I_{\text{th}}}\right)^2}\tau^{-2}$$

$$+ \frac{\frac{16\pi}{\omega^3}\frac{kT\mu_0^2\eta}{\hbar^2V_c}Q_c\left[1 + q\left(\frac{I}{I_{\text{th}}}\right)\right]^2}{-1 + (1 - 3q)\frac{I}{I_{\text{th}}} - 2q^2\left(\frac{I}{I_{\text{th}}}\right)^2}\tau^{-1}$$

$$+ \frac{4Q_c^2}{\omega^2}(\gamma_w + \gamma_b)^2\left[1 + q\left(\frac{I}{I_{\text{th}}}\right)\right]^2\sigma_c^2(\tau). \quad (3)$$

Here

$$\frac{1}{Q_c} = \frac{1}{Q_0} + \frac{1}{Q_{\text{ext}}}$$

where Q_0 is the unloaded Q of the resonator and Q_{ext} represents the loading due to external systems coupled to the cavity. This load should be as nonreactive as possible so as to avoid excessive mistuning of the loaded system by external variations.

Authorized licensed use limited to: University of Maryland College Park. Downloaded on November 29,2021 at 12:22:24 UTC from IEEE Xplore. Restrictions apply.

In a typical maser q is about 0.07 and the relationship between actually measured stability and the stability predicted from operating parameters has been accurately tested [10].

The benefits of low-temperature operation are vividly apparent in the makeup of the parameter q, which contains the factor $\sigma \bar{v}_r$. At very low temperature this factor decreases by a factor of about 10^3 from the room-temperature value. For a given maser configuration and assuming γ_w is negligible, we see that we can reduce Q_c very substantially and still, under very cold conditions, maintain the same oscillating condition represented by q. Cavity Q reduction is best done by *over*coupling the cavity resonator to the external load, thus delivering considerably more power to the load. A further advantage results from the reduced cavity pulling (provided the load is nonreactive and stable). The increased power substantially improves the stability. When the reduction in kT is included in the signal-to-noise ratio, we anticipate even further improvement in stability.

The line Q is also affected by reducing the temperature. Q_l is defined by $Q_l = \omega/2\gamma_{2T}$, and $\gamma_{2T} = \gamma_b + \gamma_w + \gamma_{se}$. We note that all three terms of γ_{2T} depend on velocity and hence on T as follows:

- $\gamma_b = \bar{v}A_e/4\kappa V_b$ is the escape rate term, where A_e/κ is the exit aperture area divided by the kappa factor [13] of the bulb collimator;
- $\gamma_w = \bar{v}p/\lambda$ is the wall relaxation term. Here λ is the mean-free distance of the atoms in the storage volume and p is the probability per collision of the atom losing phase with respect to the RF magnetic field; and
- $\gamma_{se} = n\bar{v}\sigma$ is the spin–exchange term, which has already been discussed and is included in terms of q and I in (2).

We see that simply because the atom's velocity is reduced and because the spin–exchange cross section is much smaller, lowering the temperature can improve the atomic Q provided the wall collision dephasing term is very small compared to the other terms.

II. Liquid Helium Wall Coatings

In 1979 Silvera and Walraven [14] at the University of Amsterdam, demonstrated long-term stabilization of a moderate density of atomic hydrogen at low temperature. A critical requirement was coverage of all confining walls with a film of liquid ^{4}He (which is superfluid). This inert wall coverage provides an almost ideal surface for a hydrogen maser. Subsequently, Greytak, Kleppner, and his colleagues at the Massachusetts Institute of Technology (MIT) and the Amsterdam group succeeded in obtaining magnetically confined densities as high as $10^{17}/\text{cm}^3$ in the neighborhood of 0.3 K [15], [16]. Parallel work at the University of British Columbia by Berlinsky and Hardy [17] with closed cells at very low magnetic fields demonstrated the feasibility of making transitions between the magnetic resonance hyperfine levels of the hydrogen atoms. These experiments provided a great deal of information on the interactions of atomic hydrogen on the fluid helium surfaces and in the helium gas over the surfaces. The prospects for applying helium wall surfaces have been described by Hardy and Morrow [18] and by Berlinsky and Hardy [11], who showed that the wall shift and pressure shift are both negative, reducing the transition frequency. They found that the combined wall and pressure shift has a maximum (is least negative) around 0.5 K so that operation in this region can be made stable with respect to temperature variations.

Successful oscillation of hydrogen masers at very low temperatures has been reported by both the MIT [19] and the University of British Columbia groups [20]. Parallel efforts to design, build, and operate a low-temperature maser at Harvard have been rewarded by successful oscillation [21].

III. The Harvard–Smithsonian Cryogenic Hydrogen Maser

We have designed, built, and demonstrated operation of a cryogenic maser (CHM) operating in the temperature range of 350–600 mK. Our maser design is similar to that of a conventional room-temperature maser, except that the atomic hydrogen beam is cooled to low temperature, and the resonator consists of a dielectrically loaded cylindrical cavity made of sapphire [22]. A novel feature is a continuously flowing superfluid helium film that covers the maser storage volume walls to prevent recombination of the hydrogen atoms and preserves the phase of their oscillating dipole moment. This film is eventually adsorbed by a large sorption pump operating at 6 K. The CHM has been predicted by Berlinsky and Hardy [11] to have frequency stability in the range 10^{-18} for averaging times of about 10^3 s. Although room-temperature hydrogen masers have been operated with stabilities [23] of a few parts in 10^{16}, their accuracy is limited to several parts in 10^{13} by the irreproducible wall shift of Teflon surfaces. Preliminary performance results of our maser, which has been designed to yield the high predicted stability, are reported here.

Our maser is shown in Fig. 2. Atomic hydrogen in all four hyperfine states flows out of a room-temperature microwave discharge into the cryostat through a Teflon-lined tube and is thermalized by a 3-mm-diameter source aperture at 10 K, as described by Walraven and Silvera [24]. The cold beam then enters a 1.3-cm-long hexapole magnet that focusses atoms in the ($F = 1$, $m_F = 0$, and $m_F = 1$) hyperfine states into the aperture of the cylindrical dielectrically loaded microwave cavity. An axial beam stop at the exit of the hexapole magnet prevents undeflected atoms from entering the cavity. The cavity is mounted in good thermal contact within a large copper isothermal chamber that is suspended from the mixing chamber of a dilution refrigerator and can be cooled down to about 300 mK. In order to attenuate the earth's mag-

Authorized licensed use limited to: University of Maryland College Park. Downloaded on November 29,2021 at 12:22:24 UTC from IEEE Xplore. Restrictions apply.

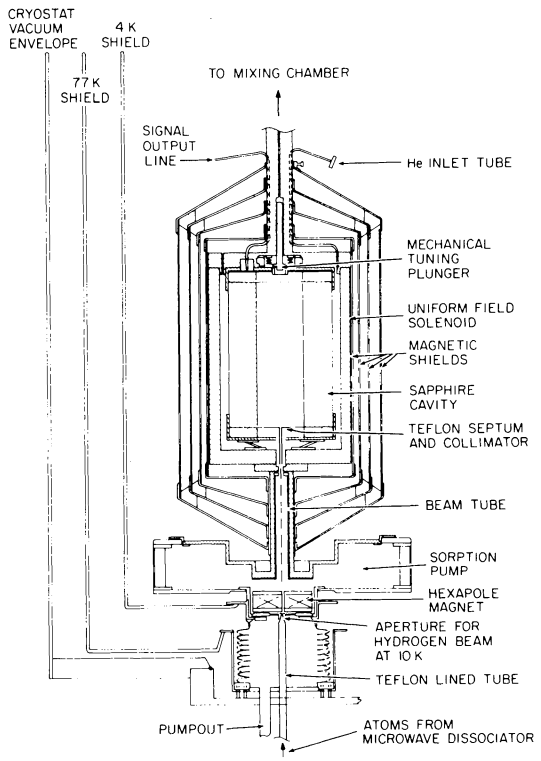


Fig. 2. Schematic diagram of the cryogenic hydrogen maser.

netic field and achieve high frequency stability the cavity is surrounded by a four-layer nested shield made of Cryoperm®, a material with high magnetic susceptibility at low temperatures. These shields operate at 4.2 K and are thermally isolated from the cavity. A uniform axial magnetic field of a few milligauss is produced in the storage volume by a solenoid made up of three separately energized coils. The solenoid is located outside the copper cylinder and within the innermost magnetic shield. A two-loop transverse coil (not shown) is attached to the wall of the microwave cavity. It is used to measure the cavity field by inducing audiofrequency $\Delta m_F = +1$ transitions that are detected by quenching of the maser oscillation. Another coil, mounted outside the beam tube between the hexapole and the cavity aperture, provides a small static "holding field" to prevent depolarization of the state-selected beam due to Majorana transitions.

The resonant cavity consists of three pieces of c-cut single-crystal sapphire. The central cylindrical section has an axial hole through its length that forms the hydrogen storage volume. The cylinder is capped by two annular sapphire discs. The interior of the cylinder is coated with Teflon for tests at higher temperatures [23] and the discs are separated from the cylinder by Teflon septa. The cavity's electrically conducting surfaces are cup-shaped copper plates at the top and bottom, and thin copper shim stock tightly wrapped around the cylinder. A Teflon tube (4 mm id and 27 mm long) passes through the lower septum to admit hydrogen atoms into the storage volume. By confining the atoms to a region where the microwave field is uniform, rather than allowing them to occupy the ends of the cavity, the septa improve the filling factor. The dimensions of the Teflon tube determines the storage time of the atoms in the cavity, which is calculated to be 7.5 s at 0.5 K. The cavity frequency can be mechanically tuned over a 600-kHz range with an externally operated cylindrical plunger. This allows us both to tune the cavity to resonance and to measure the atomic linewidth, or line Q, by detuning the cavity from resonance and measuring the ensuing maser frequency shift. The cavity is weakly coupled to a 50-Ω output coaxial cable by a pickup loop near the end of the cavity. The cavity Q is about 20 000 at room temperature and increases to 65 000 at low temperature. Due to the temperature dependence of the sapphire's dielectric coefficient, the cavity frequency increases by about 12 MHz in cooling from room temperature to 4 K. Preliminary measurements enabled us to size the sapphire so that at about 0.5 K the cavity frequency can be tuned to the hydrogen maser transition frequency of 1 420 405 751 Hz.

In order to prevent recombination of hydrogen at subkelvin temperatures, all surfaces must be covered by a film of liquid helium [14]. Since the ^{4}He is superfluid at the CHM operating temperatures, it flows to cover all surfaces, but in particular it is driven to warmer regions. Helium from a room-temperature source of variable pressure is introduced into the cavity via a capillary tube. Without proper measures the liquid helium would flow out of the cavity aperture and up the outer walls to warmer regions where it would vaporize, destroy the vacuum, and warm the dilution refrigerator to high temperatures. We have built a giant sorption pump between the beam tube and the hexapole magnet. The pump chamber is filled with activated charcoal that is thermally linked to the pump's bottom plate at 6 K. The top plate operates at the maser temperature and is thermally isolated from the bottom plate by a 25-μm thick Kapton wall. The two plates are structurally strengthened by six tubes of G-10 fiberglass-reinforced epoxy. The helium film vaporizes at the Kapton walls and, due to baffles, the vapor is cryopumped before diffusing back to the central region, where it would attenuate the hydrogen beam.

At higher temperatures, of order 550 mK, the vapor pressure of a saturated film of helium is high enough that it ordinarily would attenuate the beam in the beam tube region, reducing the population of $F = 1$, $m_F = 0$ state atoms below the threshold for oscillation. To prevent this, we have built a novel "dynamic" helium pump. Since the vapor pressure of very thin films of helium is substantially lower than the saturated value, we have placed a large number of concentric sheets of copper foil in the beam tube areas so that the helium film that flows out of the cavity aperture is subdivided into a large number of thin undersaturated films with a low vapor pressure that flow in parallel along the sheets. In addition, the cryopumping

®Registered service mark of VACUUMSCHMELTZ Gmbh., Hanau, Germany.

Authorized licensed use limited to: University of Maryland College Park. Downloaded on November 29,2021 at 12:22:24 UTC from IEEE Xplore. Restrictions apply.

copper surfaces also adsorb helium that flows out of the aperture in the vapor phase. Our current tests of the performance of the dynamic pump are inconclusive.

IV. Measurements

We have observed maser oscillation of our CHM from approximately 350–575 mK at power levels up to 5×10^{-13} W. Due to technical cryogenic problems we were unable to make measurements for periods longer than about 3 h; more important, we were limited to helium flow rates that we estimate are lower than those required to achieve saturated films. (We assume the film thickness to be essentially proportional to flow rate until the film is saturated.) As a consequence, in this article we concentrate on the relationship between the film thickness and both the maser frequency (i.e., the wall shift) and the linewidth or line Q, which is important for the frequency stability of the maser. The predicted frequency shifts from helium surface and bulk gas effects are shown in Fig. 3, along with the mean free path of hydrogen in the helium vapor.

The flow rate is determined by the pressure p, in a room-temperature helium reservoir. Because the helium supply system operates in the regime of viscous flow and the flow is therefore proportional to p^2, film thickness should also be proportional to p^2. In Fig. 4 we show the wall shift Δf_w (that is, the shift of the maser frequency from the value it would have for free atoms in the absence of walls) as a function of p^2 at a constant temperature of 0.493 K. At this temperature the wall shift for saturated surfaces is expected to be on the order of 0.1 Hz. At very small values of flow the wall shift is substantial and decreases toward the saturated value as flow or film thickness increases. This is reasonable, as for thinner films the hydrogen atoms see the more polarizable substrate [25] and we would expect the hyperfine frequency to decrease.

Fig. 5 shows the wall shift as a function of temperature for fixed helium flow rates. For a saturated film this curve is expected to be bowl shaped, the shift decreasing as temperature increases to about 0.6 K and then increasing at higher temperatures due to the pressure shift. Our data, which are for $T < 0.6$ K, are consistent with this behavior. In Fig. 5 we also show the line Q as a function of temperature for fixed helium flow rates. If the line Q is limited only by the cavity escape time (7.5 s), then we expect $Q_l = 3 \times 10^{10}$. The measured values of Q_l are much smaller than the calculated value, but increase rapidly with temperature and, more important, with helium film thickness. In order to characterize the CHM as an oscillator of extreme frequency stability, it will be necessary to extend these measurements to saturated values of helium film.

V. Conclusion

The stability we expect to observe, assuming the performance indicated by (3), is shown in Fig. 6 as the lower dotted curve. The currently available stability of the SAO VLG-11 masers is shown in a solid line, as is the stability

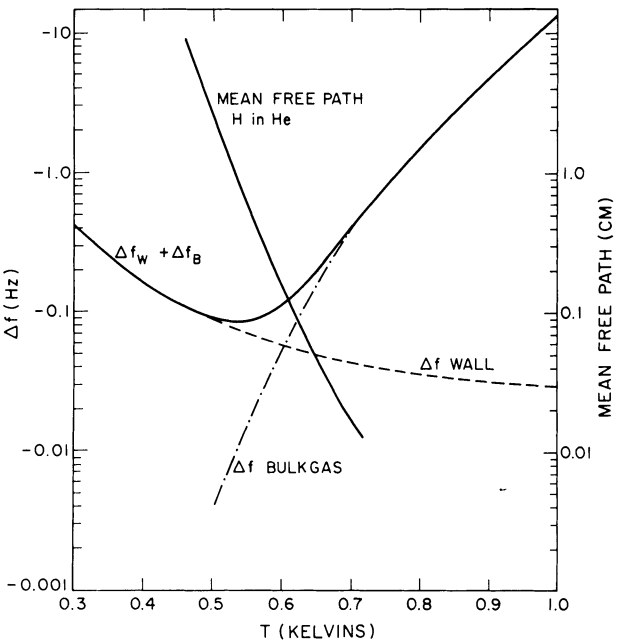


Fig. 3. Predicted frequency shift and mean free path for hydrogen in the cryogenic maser as a function of temperature.

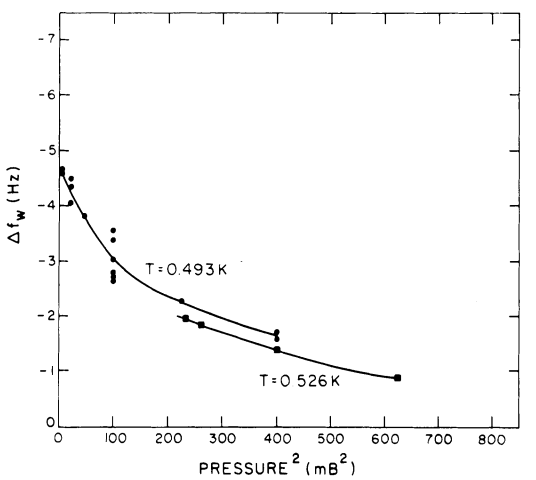


Fig. 4. Measured wall shift in the cryogenic maser versus (pressure)^2 in the viscous flow region of the helium supply system.

of the Hewlett-Packard mercury ion standard [26]. The projected stability [12] of room-temperature hydrogen masers, operating with an improved atomic state selection system, is shown as a dotted curve that just touches the 1×10^{-16} level at 3×10^4 s.

We realize that there are many systematic effects capable of affecting the maser's output frequency that are very large compared to the statistically represented performance. The traditional sources of instability such as cavity-pulling and magnetic variations seem to be well within our ability to control owing to the low cavity Q, high line Q, and use of superconducting magnetic shields. The atomic hydrogen wall and bulk gas frequency shifts shown in Fig. 3, demand control of temperature at the 0.53-K nullpoint within 20 μK if 10^{-18} stability is to be achieved. This, too, is within the present state of technology [27].

Authorized licensed use limited to: University of Maryland College Park. Downloaded on November 29,2021 at 12:22:24 UTC from IEEE Xplore. Restrictions apply.

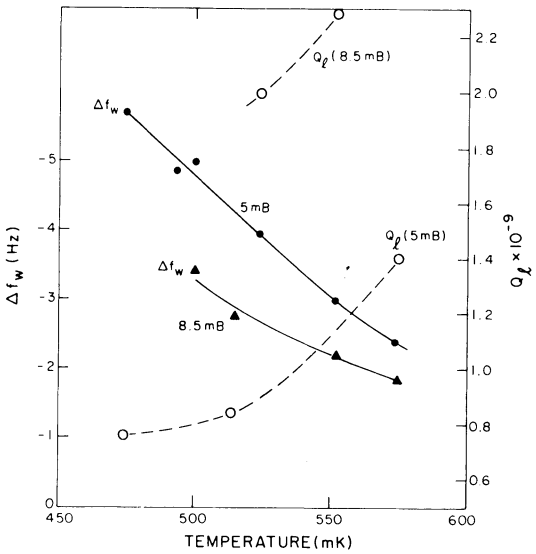


Fig. 5. Measured wall shift and maser oscillation line q as a function of temperature.

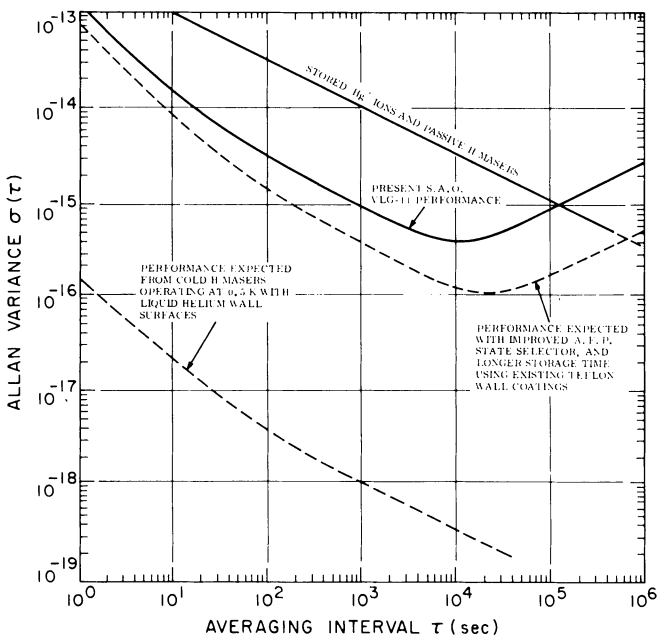


Fig. 6. Predicted frequency stability for cryogenic masers compared to that of other high-performance clocks.

So far, as we have yet to achieve a fully saturated helium film in the storage volume, we are uncertain as to the required hydrogen flow stability, let alone the stability of the flowing film itself or its dynamics as seen from the perspective of the incoming hydrogen atoms. We expect that ongoing measurements will help to resolve some of these questions and lead us to new information about hydrogen–helium surface interactions and to the development of better clocks.

Acknowledgment

The authors would like to thank P. Crevoiserat for his expert craftsmanship in building the maser. They also thank D. Graveline, R. Nicoll, and Shen-Wei for their valuable help in preparing and testing the sapphire resonator and the hexapole magnet.

References

[1] D. Kleppner, H. M. Goldenberg, and N. F. Ramsey, *Phys. Rev.*, vol. 126, p. 603, 1982.
[2] I. I. Shapiro, private communication, 1977.
[3] S. B. Crampton, W. D. Phillips, and D. Kleppner, *Bull. Amer Phys. Soc.*, vol. 23, p. 86, 1978.
[4] R. F. C. Vessot, E. M. Mattison, and E. Imbier, "Cold hydrogen maser research at SAO and related developments," in *Proc. 37th Symp. on Freq. Control*, June 1-3, 1983, Philadelphia, PA.
[5] S. B. Crampton, K. M. Jones, G. Nunes, and S. P. Souza, *Proc. 16th Annu. Precise Time, Time Interval Meeting*, 1984, p. 339.
[6] D. W. Allan, *Proc. IEEE*, vol. 54, p. 221, 1966.
[7] R. F. C. Vessot, *Quantum Electronics III*, P. Grivet and N. Bloembergen, Eds. New York: Columbia Univ., 1964, p. 409.
[8] L. S. Cutler and C. L. Searle, *Proc. IEEE*, vol. 54, p. 136, 1966.
[9] D. Kleppner, H. C. Berg, S. B. Crampton, N. F. Ramsey, R. F. C. Vessot, H. E. Peters, and J. Vanier, *Phys. Rev.*, vol. 138, p. 972, 1965.
[10] R. F. C. Vessot, M. W. Levine, and E. M. Mattison, *Proc. 9th Annu. Precise Time, Time Interval Meeting*, 1977, p. 547.
[11] A. J. Berlinsky and W. N. Hardy, *Proc. 13th Annu. Precise Time, Time Interval Meeting*, 1981, p. 547.
[12] E. M. Mattison, R. F. C. Vessot, and Shen-Wei, *Proc. 40th Symp. Frequency Control*, 1986.
[13] P. Clausing, *Physica*, vol. 9, p. 65, 1929.
[14] F. Silvera and J. T. M. Walraven, *Phys. Rev. Lett.*, vol. 44, p. 164, 1980.
[15] R. W. Cline, T. J. Greytak, D. Kleppner, and D. A. Smith, *J. Phys. Colloq.*, vol. 41, no. C-7, p. C7/151, 1980.
[16] J. T. M. Walraven, I. F. Silvera, and A. P. M. Matthey, *Phys. Rev. Lett.*, vol. 45, p. 449, 1980.
[17] M. Morrow, R. Jochemsen, A. J. Berlinsky, and W. N. Hardy, *Phys. Rev. Lett.*, vol. 46, p. 145, 1981; Erratum, vol. 47, p. 455, 1981.
[18] W. N. Hardy, M. Morrow, *J. Phys. Colloq.*, vol. 42, p. C8/171, 1981.
[19] H. F. Hess, G. P. Kochanski, J. M. Doyle, T. J. Greytak, and D. Kleppner, *Phys. Rev. A.*, vol. 34, p. 1602, 1986.
[20] M. D. Hurlimann, W. N. Hardy, A. J. Berlinsky, and R. W. Cline, *Phys. Rev. A.*, vol. 34, p. 1605, 1986.
[21] R. L. Walsworth, I. F. Silvera, H. P. Godfried, C. C. Agosta, R. F. C. Vessot, and E. M. Mattison, *Phys. Rev. Rapid Commun.*, in press.
[22] V. J. Folen, W. G. Mausch, J. D. White, C. A. Bartholomew, and A. J. Frank, *N. R. L. memo rep.* 487D, U.S. Naval Res. Lab., Washington, DC, 1982.
[23] R. F. C. Vessot, E. M. Mattison, W. J. Klepczynski, I. F. Silvera, H. P. Godfried, and R. L. Walsworth, Jr. *Proc. 17th Annu. Precise Time, Time Interval Meeting*, p. 413, 1985.
[24] J. T. M. Walraven and I. F. Silvera, *Rev. Sci. Instr.*, vol. 53, p. 1167, 1982.
[25] H. Godfried, E. Eliel, J. Brisson, J. Gillaspy, C. Mallardeau, and I. F. Silvera, *Phys. Rev. Lett.*, vol. 55, p. 131, 1985.
[26] L. S. Cutler, R. P. Gifford, and M. D. McGuire, *Proc. 37th Symp. Frequency Control*, 1983, p. 32.
[27] J. A. Lipa, Int. Conf. Low Temp. Phys., *Physica 107* B + C, p. 343, 1981.

Authorized licensed use limited to: University of Maryland College Park. Downloaded on November 29,2021 at 12:22:24 UTC from IEEE Xplore. Restrictions apply.